

A neurobiological theory of meaning in perception.

Part 3. Multiple cortical areas synchronize without loss of local autonomy

International Journal of Bifurcation & Chaos [2003] 13: in press.

Walter J Freeman*

Gyöngyi Gaál†

Rebecka Jörnsten‡

Department of Molecular and Cell Biology
University of California
Berkeley CA 94720-3200 USA
tel 510-642-4220 fax 510-643-6791

*Corresponding author: wfreeman@socrates.berkeley.edu

†Present address:
Neuroprosthesis Research Organization
GPO Station, PO Box 20350
Brooklyn NY 11202-0350
gaal@neuroprosthesis.org

‡Department of Statistics
Rutgers University
rebecka@stat.rutgers.edu

Key words: binding, gamma band, neurodynamics, phase locking, spatial EEG patterns,
synchronization

Running title: Synchrony among multicortical EEGs

ABSTRACT

Information transfer and integration among functionally distinct areas of cerebral cortex of oscillatory activity requires some degree of phase synchrony of the trains of action potentials that carry the information prior to the integration. However, propagation delays are obligatory. Delays vary with the lengths and conduction velocities of the axons carrying the information, causing phase dispersion. In order to determine how synchrony is achieved despite dispersion, we recorded EEG signals from multiple electrode arrays on five cortical areas in cats and rabbits, that had been trained to discriminate visual or auditory conditioned stimuli. Analysis by time-lagged correlation, multiple correlation and PCA, showed that maximal correlation was at zero lag and averaged .7, indicating that 50% of the power in the gamma range among the five areas was at zero lag irrespective of phase or frequency. There were no stimulus-related episodes of transiently increased phase locking among the areas, nor EEG "bursts" of transiently increased amplitude above the sustained level of synchrony. Three operations were identified to account for the sustained correlation. Cortices broadcast their outputs over divergent-convergent axonal pathways that performed spatial ensemble averaging; synaptic interactions between excitatory and inhibitory neurons in cortex operated as band pass filters for gamma; and signal coarse-graining by pulse frequency modulation at trigger zones enhanced correlation. The conclusion is that these three operations enable continuous linkage of multiple cortical areas by activity in the gamma range, providing the basis for coordinated cortical output to other parts of the brain, despite varying axonal conduction delays, something like the back plane of a main frame computer.

1. INTRODUCTION

An outstanding characteristic of neurons is the contrast between the functions of dendrites and axons. The dendrites receive signals by chemical transmitter molecules from other neurons at synapses, convert them to loop currents, and sum the potential differences at trigger zones in proportion to synaptic strength and distance along the dendritic tree. The axon converts the sum to an analog pulse rate or sequence of intervals and transmits the pulsatile signal to distances far exceeding the range of diffusion that dominates dendritic function, by calling on local energy stores to maintain the pulse amplitudes without attenuation over long distances. The cost is time delay in proportion to distance and conduction velocity that vary with axon diameter. Cortical neurons receive axons from other neurons located at many distances. The appropriate model for dendritic integration is a leaky RC network with a passive time constant on the order of 5 to 10 ms. The distribution of time delays of input can exceed this range. The problem here is to understand how linear integration by dendrites to give output can be compatible with the distributed time delays for input that are imposed by axonal conduction, when the input signals are aperiodic or have multiple characteristic frequencies. The problem holds not only for integration among widely separated areas of cortex, but also for control of brain stem nuclei by the convergence of signals from widely separated cortical areas with differing distances and different selections of areas during diverse forms of behavior. Previous efforts to solve this problem have been focused on networks with highly specific error correcting algorithms. The approach taken here is to find a general solution that holds for all areas of cortex [Freeman, 2003].

The premise on which this approach is based is that sensory information serves to destabilize the primary receiving areas and select basins of attraction that determine the spatial amplitude modulation (AM) patterns of cortical activity. The AM patterns provide the signals that are

transmitted in wave packets. The wave packets are large with respect to the sizes of cortical columns and hypercolumns, but they are small with respect to the cerebral hemisphere. Owing to their size and integration of multiple receiving areas in each modality, they are broadcast throughout each hemisphere, and beyond into the opposite hemisphere, and into the brain stem. The question here is what the mechanisms might be that govern the convergence of multiple wave packets in multiple areas as the basis for simultaneous integration by the brain as a whole. A significant step has been taken in this direction by Eckhorn et al. [2001] and Bruns et al. [2000], who demonstrated systematic coordination of the envelope of gamma activity in multiple cortical areas in association with behavior, without phase locking of the high frequency carrier waves. Widespread phase locking of gamma oscillations has been reported in scalp EEGs after narrow band filtering [Haig et al., 2000], which might result from smoothing of cortical signals by the intervening skull and soft tissues.

Wave packets have been documented so far in primary sensory areas one at a time only, so they do not constitute Gestalts (multisensory perceptions) [Freeman, 2001]. In order to search for Gestalts in the present study our limited recording resources were spread thin. A small rectangular array was placed on or in each of the 4 sensory areas for distance reception (not including taste). Most importantly, a small array was placed on that area of the limbic system, the entorhinal cortex, to which all sensory areas transmit, and which performs multisensory integration. Of the 64 electrodes, 16 were placed in high density arrays over the visual, auditory and entorhinal cortices, 14 over the somatomotor cortex, and 2 in the olfactory bulb of cats and rabbits. After the subjects were trained in sensory discrimination, the 64 EEGs were analyzed by linear techniques in search of the transient increases in covariance predicted by the linear binding hypothesis. None was found. What appeared instead was a remarkably high level of sustained covariance among the EEGs from the several areas of recording, under three constraints of data analysis. Following presentation of the results, we describe neural

mechanisms corresponding to these three constraints, that together may yield the mechanism for synchrony that is required for macroscopic pattern formation by linear integration.

2. METHODS

2.1. Subjects and tasks

Cats were selected as subjects because multiple electrodes can be fixed on the pial surface of the entorhinal cortex by sliding a 2x8 planar array along the flat upper surface of the bony tentorium from the dorsolateral edge of the occipital cortex to the depth of the temporal fossa. Also, cats were more amenable than rabbits to operant appetitive conditioning [Gaál & Freeman, 1998], the neurodynamics of their olfactory gamma activity had been modeled [Freeman, 1975], and the connections of the entorhinal cortex had been well studied in cats [Boeijinga & Lopes da Silva, 1988; Lopes da Silva et al., 1990] and other species [Buszáki, 1996; Kay & Freeman, 1998; Ahrens & Freeman, 2001]. Four female cats aged 42, 19, 8 and 8 months were implanted under aseptic surgery with 3 arrays of 14-16 stainless steel (0.25 mm) wire electrodes (0.8 mm apart, 3x3 mm on the convexity) fixed in the left cerebral hemisphere epidurally over the posterior sigmoid gyrus, the midectosylvian gyrus, and the posterior lateral gyrus, and a 2x8 array subdurally on the entorhinal cortex (0.8 x 1.5 mm apart, 1.6 x 6.4 mm), plus 2 depth electrodes, one in the bulb and the other close to its dorsal surface. Reference electrodes were placed over the right frontal sinus and right superior orbital buttress, and ground electrodes were connected to screws set in the posterior skull to stabilize the dental acrylic mounting for attaching the 64 monopolar recording leads and 5 reference and ground leads to Amphenol connectors fixed to the calvarium. Buprenorphine and Baytril antibiotic were given for 5 days postoperatively. Placements were verified by dorsal and lateral x-rays postoperatively and again after sacrifice (120 mg/kg pentobarbital intravenously followed by perfusion with artificial CSF and 10% formalin) and dissection to check for possible re-growth of bone and cortical damage. All procedures were in accordance with NIMH guidelines and under close supervision by the Berkeley Campus Animal Care and Use Committee and its veterinary staff.

Familiarization was followed by training first to visual (3.6 vs. 2.8 ft.-cd full field flashes) and then to auditory (500 vs. 5,000 Hz pure tones for 0.1 s ~20 db above background white noise) discriminative conditioned stimuli (CS) for 3 of the 4 cats (labeled S1, S2 and S4 in Fig. 2), and to auditory CS for the other cat (S3). The CS intensities were adjusted so that the peak amplitudes of the evoked potentials were close to those of the background EEGs. Subjects were trained to hold the bar down in anticipation of each trial, which started with a brief warning flash and lasted 6 s with 3 s control and 3 s poststimulus periods. Intertrial intervals were 12-60 s. Reinforcement of a correct conditioned response (CR, bar release) following a reinforced conditioned stimulus (CS+) was an aliquot of soft food delivered by a peristaltic pump, if the subject responded between 0.35 and 2.65 s of stimulus onset. The penalty for responding too soon, too late, or to an unreinforced conditioned stimulus (CS-) was an additional delay of variable duration. A session consisted of 20 trials each of artifact-free records with CS+ and CS- on randomly interspersed trials. After completion of training and recording a set of 10 sessions was selected for intensive analysis from the best performances: 3 each from S1 and S4, and 2 each from S2 and S3.

2.2. Recording and time series analysis

EEGs were recorded monopolarly from that one of 2 or 3 reference electrodes contributing the lowest level of EEG activity, amplified 10K with analog pass band 0.1-100 Hz, digitized (12 bits, 10 microsec per channel, sample interval 2 ms over 63 EEG channels and 1 CR channel. Signals on up to 4 bad channels including that with the CR marker were replaced with adjacent signals. FFT, coherence, and time-lagged crosscorrelation were calculated on 64-512 ms epochs in time windows stepped variously at 32-256 ms. Averages and standard deviations (SD) of temporal properties were calculated over 20 blocks of EEGs from cats at rest, 20 CS+ trials, and 20 CS- trials. Crosscorrelation, multiple correlation, and principal components analysis (PCA) were done after band pass filtering and spatial ensemble averaging. Initially the pass band was

set at the optimal range for spatial AM pattern classification in rabbits, 20-80 Hz [Barrie, Freeman & Lenhart, 1996], and then it was optimized for cats using the same criterion of optimal AM pattern classification. The ensemble of signals for spatial averaging was taken from the cluster of electrodes on each sensory area. The 95% confidence intervals of linear time-lagged crosscorrelation coefficients were estimated by the standard method after prewhitening with a simplified AR model [Brockwell & Davis, 1991], which necessarily was updated for each epoch owing to nonstationarity. To estimate the uncertainties after filtering and averaging, the stationary bootstrap method of Politis, Romano & Lai [1998] was used. This method re-samples random length blocks of data and creates pseudo-data with component structure similar to that of the EEG data, somewhat similar to jack-knifing [Freeman & Grajski, 1987] and to constructing shuffled EEG data [Freeman & Rogers, 2002].

3. RESULTS

3.1. Spectral analysis and pair-wise correlation of multiple cortical EEGs

The EEGs were displayed after editing for artifacts [Fig. 1]. The signals within each area conformed in shape, but differed in amplitude. PCA was applied to the 12-16 signals from each area in the moving window across all trials for each subject. The percentage of the total variance taken by the 1st component was seldom less than 95%. In contrast, the signals from multiple areas differed in both mean amplitudes and wave forms. PCA was applied to all 64 signals from the 5 areas, on the assumption of zero time lag for the first component. The percentage of variance in that component varied inversely with window duration: 64 ms, $60.1 \pm 8\%$; 128 ms, $57.2 \pm 7\%$; 256 ms, $55.1 \pm 7\%$. Power spectral densities of representative signals [Fig. 2] were approximately $1/f^\alpha$ in log-log coordinates, which was typical of neocortical though not of olfactory EEGs [Barrie, Freeman & Lenhart, 1996]. The mean slope of α was -1.96 ± 0.31 (SD). Spectral peaks revealed power above the regression lines in the gamma and theta ranges of spectra from the bulb and to a slight extent the somatomotor cortex but not in the other neocortical EEG spectra. In these respects the EEGs from cats did not differ significantly from EEGs recorded from the same areas in rabbits with multiple 4x4 arrays or with an 8x8 array in each subject on only one area.

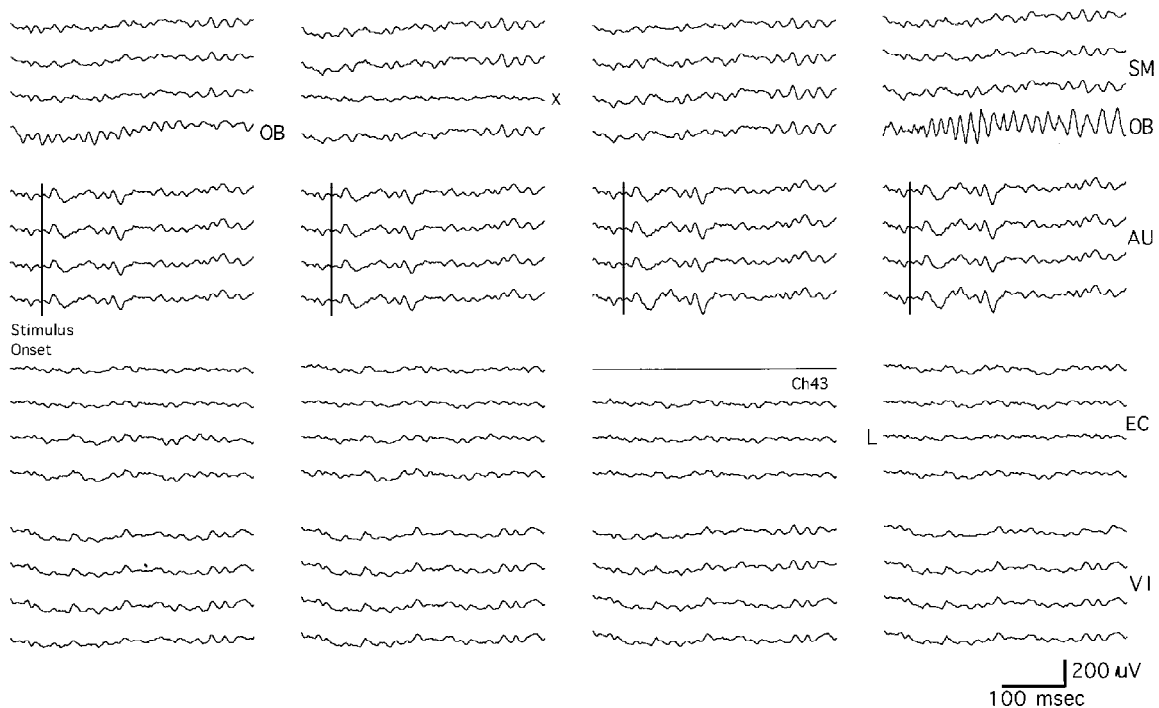


Figure 1. A 400 msec segment is shown of 64 simultaneous recordings with analog pass band 0.1-100 Hz, digitized at 2 msec intervals (10 microsec between channels), and grouped by areas (SM, somatomotor; OB, olfactory bulb; AU, auditory cortex; EC, entorhinal cortex; VI, visual cortex). Channel 43 was used to record the CR. The 'x' indicates a bad channel. The 'L' indicates the channel with lowest amplitude, by which to judge the maximal fluctuations that could be attributed to the monopolar reference electrode. The vertical line across the auditory EEGs indicates the time of onset of a 500 Hz tone for 0.1 sec, which was followed by the 'on' and 'off' unaveraged evoked potentials.

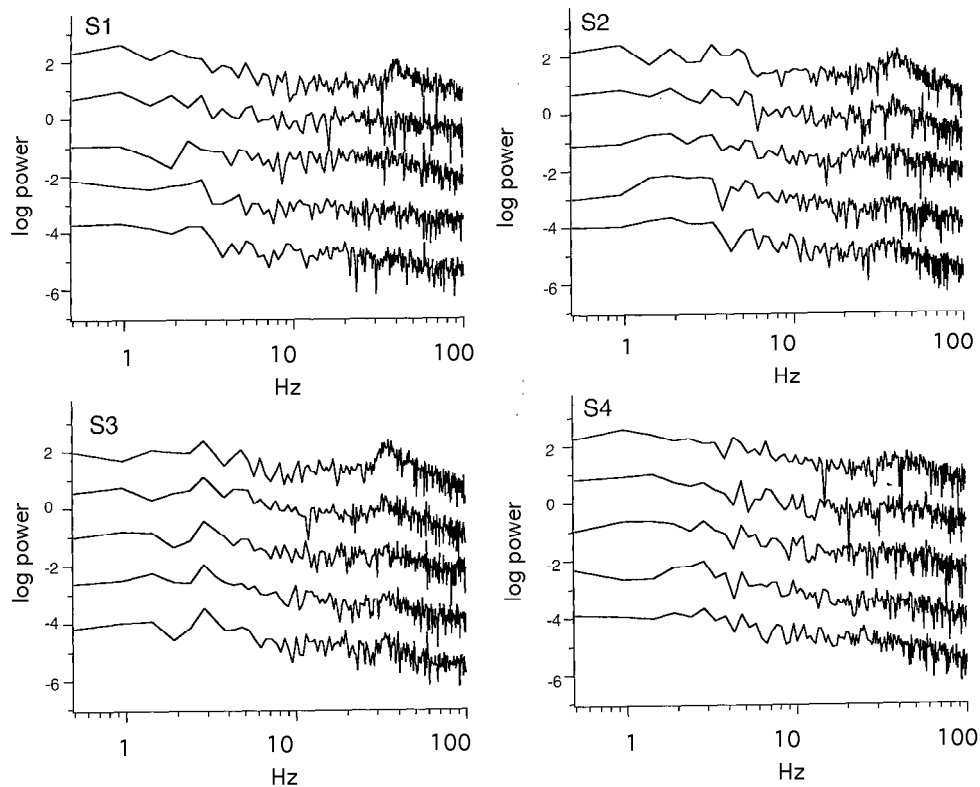


Figure 2. Power spectral densities are shown in log-log plots for the 4 subjects and the 5 areas, from top to bottom: OB, SM, AU, VI and EC. Strong power in the gamma range was observed in olfactory EEGs of cats S1, S2 and S3, and less so in somatomotor EEGs of cats S2 and S3. There was no excess gamma power in the auditory and visual cortical spectra of cats S1 and S4.

The question was posed whether phase relations between gamma waves from pairs of cortices might reveal transient episodes of phase stabilization or convergence to zero phase differences between the sensory areas receiving the CS and other areas, particularly the entorhinal cortex, at times between the CS and CR onsets, with or without increases in EEG amplitudes ('bursts'). Pairwise calculation of intercortical cospectral densities in moving windows stepped through the control and test periods revealed sustained high values of coherence amplitude corresponding to the zero-lag correlation coefficients, and with phase values varying around zero in the range of $\pm 23^\circ$, as previously found within electrode arrays in rabbit data [Freeman, 2000a; Freeman & Barrie, 2000]. No significant temporal fluctuations in coherence were found coinciding with behavioral time markers.

Episodes of increased correlation were sought at zero lag and at lags corresponding to transmission delays estimated from published values of corticocortical axonal conduction velocities, the distances between arrays, and the peak frequencies of the gamma oscillations [Freeman, 2000b]. Time-lagged crosscorrelation values were computed from intercortical pairs of EEGs in overlapping 128 ms windows stepped at 100 ms intervals, with time lags stepped at 2 ms intervals between signals to ± 38 ms, after band pass filtering (20-80 Hz) of pairs of normalized spatial ensemble averages of EEGs from the multiple areas [Fig. 3]. As a control the procedure was repeated on shuffled data after randomization of the phases of the raw data, and on sets of random numbers that were generated as independent time series, digitized, filtered, and spatially ensemble averaged in the same way as the sets of EEGs. Visual inspection of representative spatial ensemble averages from multiple areas, normalized in amplitude over the entire trial length and superimposed [Fig. 4], showed no episodes of phase convergence between the carrier waves, particularly not in relation to the onsets of CS or CR. Similar results appeared in the noise control data [Fig. 5], in which random numbers were generated in 64 independent time series, truncated as in analog-to-digital conversion at 12 bits, spatially ensemble averaged in 5 groups, band pass filtered as with EEG, normalized, and superimposed. Fig. 5 shows the structure that was imposed on the random numbers by these three operations.

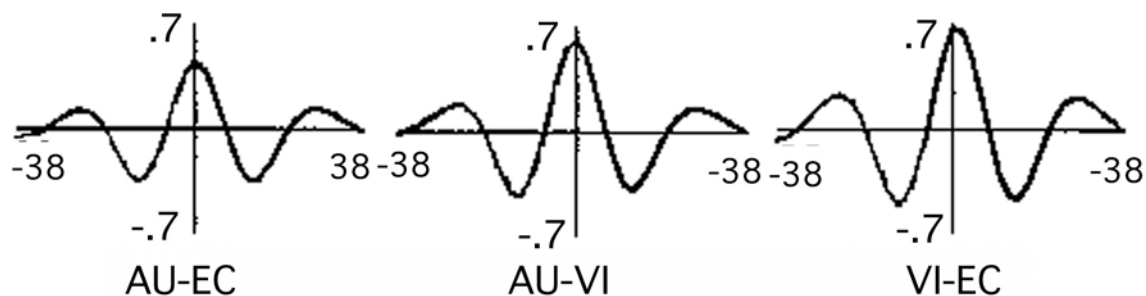


Figure 3. Examples are shown of time-lagged correlations, that were calculated between ± 38 msec from the regional spatial ensemble averages after band pass filtering. The values revealed maximal peaks up to 0.7 at zero lag, and lesser peaks at lag times corresponding to the wave length of the middle of the gamma range, here 20-80 Hz.

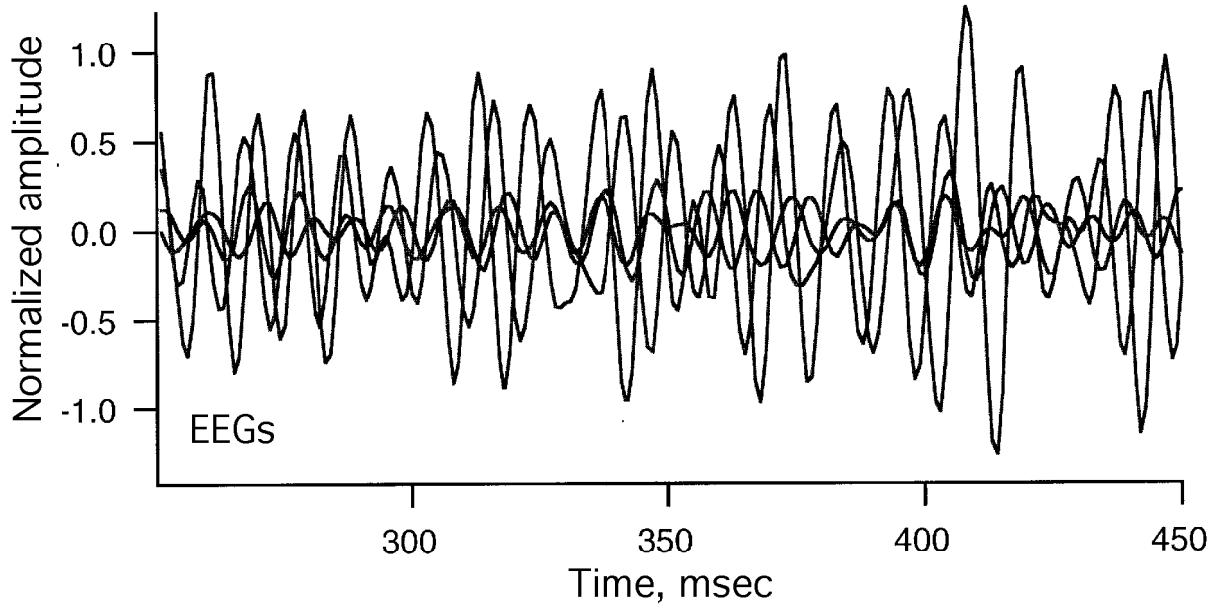


Figure 4. Spatial ensemble averages (SEA) in a 400 msec segment of simultaneously recorded EEGs from OB, SM, AU, VI and EC from a single trial have been superimposed to show the similarity of wave forms imposed by band pass filtering (here 35-60 Hz) in the range that gave optimal AM distribution classification after normalization of amplitudes of each SEA over the entire 6 sec trial. Differences in amplitude in this segment reflect slow variations in amplitude of each channel over the trial, reflecting that 'burst' amplitude of the ensemble had no significance. No episodes of apparent phase convergence occurred, particularly not in relation to CS onsets nor to times of AM spatial pattern classification.

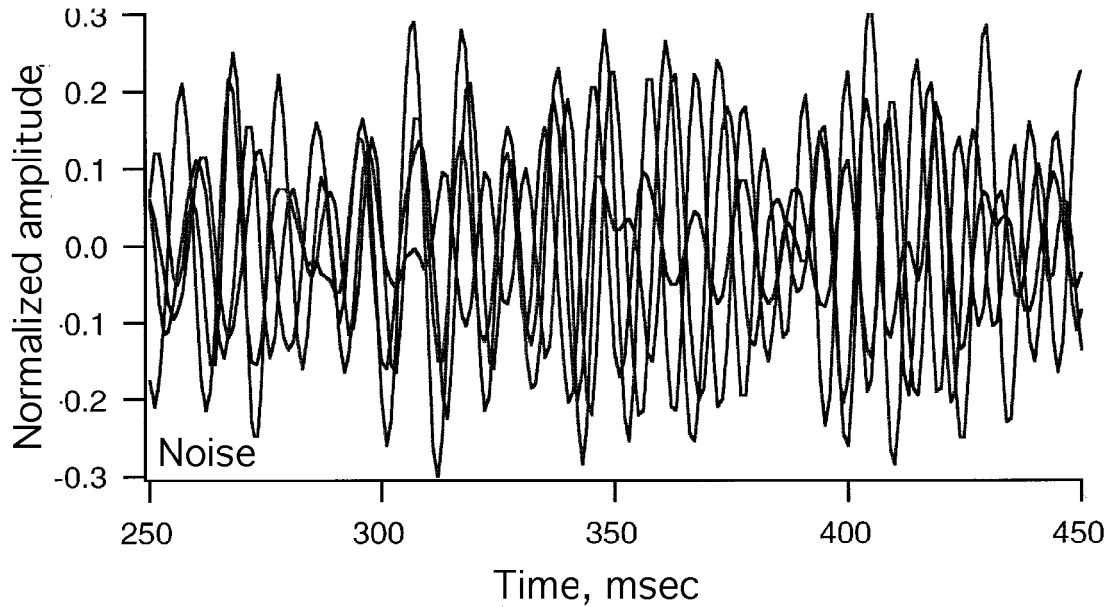


Figure 5. Normally distributed random numbers with zero mean and unit standard deviation were generated as 64 independent traces, 'digitized' (truncated) to 12 bits, spatially averaged in 5 clusters of 2 to 16, normalized in amplitude over a 6 sec segment, filtered (35-60 Hz), and superimposed as was done with EEGs. The mean correlation between the EEGs at zero lag (0.72) was lower than that of the colored noise traces (0.46), but neither was statistically significant after pre-whitening. The apparent higher frequency of the oscillations compared to the EEGs in the same pass band is due to the fact that the filtered noise was not weighted in the $-1/f^2$ relation.

In respect to time-lagged correlation, maximal values occurred at or near zero lag (± 2 ms) throughout trials [Fig. 3]. Secondary peaks at lags near ± 22 ms in bulbar and somatomotor EEG data corresponded to the center frequency (45 Hz) of the gamma peaks in the spectral pass band. Peaks of correlation at zero lag also emerged from shuffled and noise data though with lower correlation coefficients. In contrast, correlations between pairs of signals from two cortices in these subjects without spatial averaging did not show these high levels [Kozma et al., 2001].

3.2. Principal components analysis and multiple correlation

Digitizing, spatial ensemble averaging and band pass filtering were necessary to identify and measure the properties of the gamma EEG. These operations on the data required bootstrap techniques for evaluating the statistical significance of crosscorrelation values. An example is shown in Fig. 6 of the time-lagged crosscorrelation between the spatial ensemble averages from the auditory-entorhinal pair, with a 256 ms (128 bins) epoch centered at 3000 ms and stepped ± 20 ms at 2 ms (1 bin). The same results were obtained with other intercortical pairs and with samples centered at 1600, 2400, 3200, 3600 and 4000 ms, and with time-windows of 128 and 512 ms. The vertical bars show the correlation values at 2 ms steps with maximal values at or near zero time lag (± 1 bin). The horizontal dashed lines show the standard 95% confidence interval. The fluctuating curves show the confidence intervals after prewhitening with AR models and bootstrapping to compensate for the structure imposed by band pass filtering. The validity of these procedures was verified by the near congruence of the standard and bootstrap confidence intervals when band pass filtering was omitted [Fig. 7]. Notable results were the lack of statistical significance of crosscorrelation values for EEG signals after band pass filtering, particularly the high value at zero and the negative values near ± 10 ms close to the half wave length of the center frequency of the band pass filter, and the significant correlation commonly found at zero lag in unfiltered data, which could be explained by the high amplitude of low frequency activity found in all pairs, in conformance with the $1/f^\alpha$ power relation.

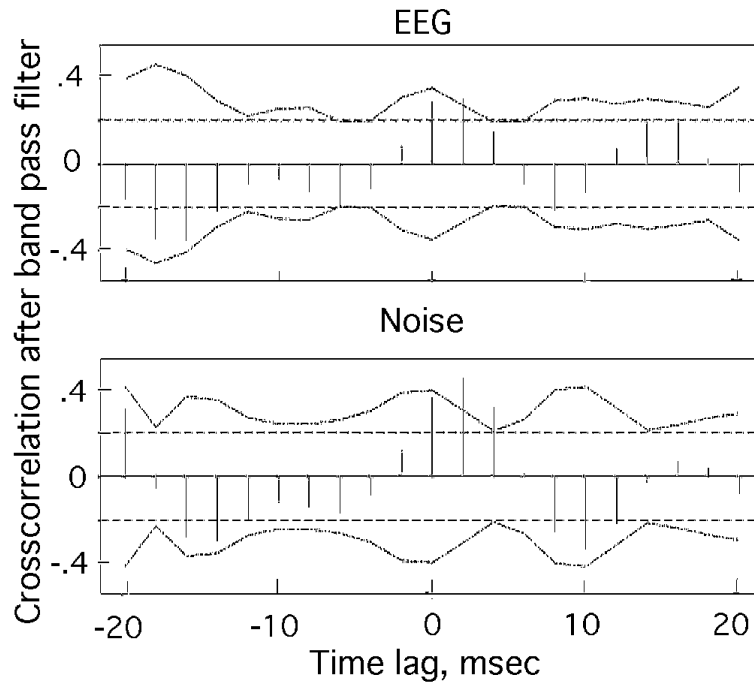


Figure 6. The results are shown of time-lagged crosscorrelation between auditory and entorhinal EEGs after band pass filtering in the gamma range (here 20-80 Hz) and local spatial ensemble averaging (upper frame). They are compared with the results of applying the same procedures to random number time series (lower frame). The straight dashed lines give the 95% confidence intervals from the standard method. The dashed curves show the 95% confidence intervals that were derived by using AR models for prewhitening and the bootstrap method.

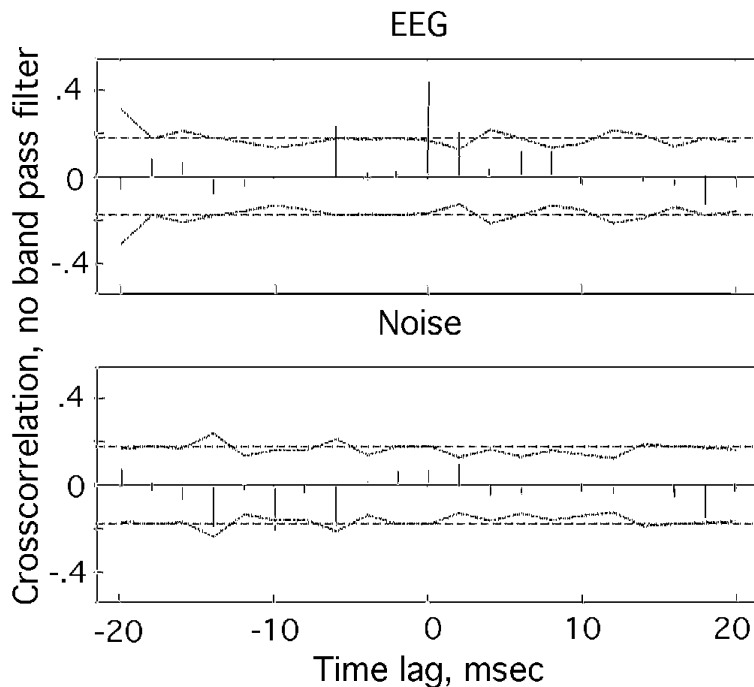


Figure 7. The same data as in Figure 4 were analyzed in the same way but without the band pass filter. The close similarity of the confidence interval from the bootstrap method with that of the standard method showed that the correlations were in large part but not completely due to the band pass filter.

On the basis of the finding of maximal pairwise correlation at zero lag, PCA was applied in stepped windows to the 64 signals. The mean levels of % variance incorporated by the 1st component varied between subjects from 50-80% over the trial sets [Fig. 8]. In no case was there sustained evidence of transient increase or decrease in % variance reliably in relation to behavior, nor were transient increases in amplitude ('bursts') found. Multiple correlation coefficients, R , were calculated at zero lag using the local spatial ensemble averages of the EEG signals from the four primary sensory areas to predict the spatial ensemble average of the EEGs of the entorhinal cortex as the dependent variable. The mean value from 128 ms overlapping windows stepped along the trial data was $\sim 0.75 \pm 0.02$. Its squared value was consistent with the fraction of the variance in the 1st component of PCA ($R^2 \sim 0.57$). No peaks in R were seen in the CS and CR intervals [Fig. 9], particularly at times when augmented phase coherence between a primary sensory area and the entorhinal or somatomotor cortices might have been predicted following reception of an appropriately directed CS.

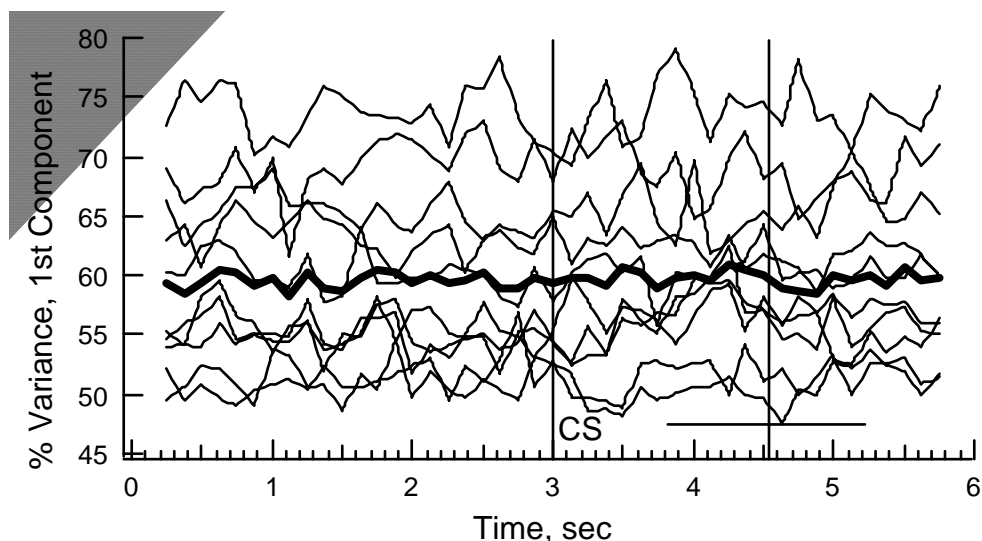


Figure 8. The loading factor of the dominant component of the PCA fluctuated about a different level for each subject and session, but showed no peaks with respect to behavioral markers. The dark trace is the mean. The vertical lines show the time of onset of the CS and the mean reaction time for the CR. The horizontal bar indicates the SD.

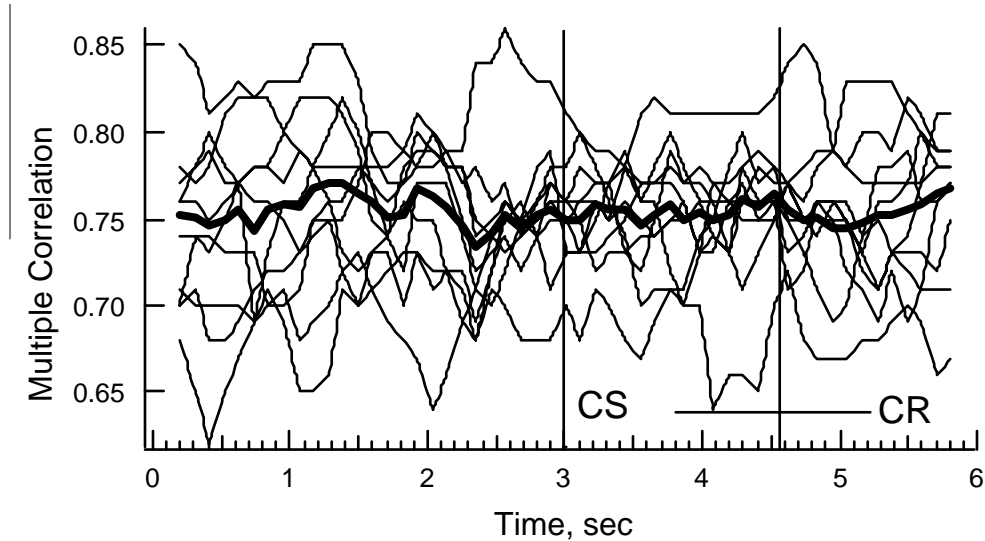


Figure 9. An example is shown for one session of the multiple correlation coefficient, R , calculated with the EEG of the entorhinal cortex as the dependent variable to be predicted by the four sensory EEGs. Values were averaged over 40 trials. No significant changes were found in the test period as compared with the pre-stimulus control period. The dark trace is the mean.

4. DISCUSSION

4.1. Integration by phase locking at single frequencies: the linear binding hypothesis

Widely distant cortical neurons create spatiotemporal patterns of activity by coordinating the timing of their action potentials. Propagation imposes time delays that depend on the distances between neurons and the diameters of axons. Cognitive function requires participation of millions of neurons and tens of millions of action potentials that are formed into rapidly changing patterns. The changes may involve cortical locations that differ from one pattern to the next. The time-variance of locations compounds the problem of how so many neurons can coordinate their firing to make the patterns. Most prior efforts to understand the coordination of timing have addressed the action potentials directly, on the premise that the intensity of cortical transmission depends on both mean firing rates and the degree of synchrony among precisely timed pulse trains [Stryker, 2001]. The present study addresses extracellular dendritic potentials, which are correlated with local densities of action potentials from many neurons [Freeman, 1975; Eeckman & Freeman, 1990]. This reorientation shifts the focus of analysis from pulse trains to local mean fields, leading to a hypothesis of global communication in the forebrain through integration of oscillatory pulse densities that are converged from multiple populations.

Local neighborhoods in cortex display EEG oscillations in several frequency ranges. The degree of synchrony in oscillation at any one frequency can be expressed by the variance of the phase distribution over multiple samples from simultaneous recordings. An increase in synchrony is signified by a decrease in variance, which may indicate an increase in 'binding' among participating neurons. This linear 'binding hypothesis' was conceived from EEG studies in the olfactory system [Fig. 9 in Freeman, 1979] and from unit studies and psychophysics in the visual system [Milner, 1974; von der Malsburg, 1983; Singer & Gray, 1995]. By hypothesis, the phase distribution of multiple EEGs and/or pulse trains, that were triggered by a multi-featured stimulus, would collapse toward 'zero lag' during an act of perception. The operation was linear vector summation, because the common frequency at which the multiple neurons oscillated and

sum their outputs would be conserved. If that frequency were determined by the input from a distant transmitter, then there would be a brief local event of increased coherence. A phase delay between transmitter and receiver was predicted, which would be determined by the carrier frequency, the transmission distance, and the conduction velocity [Freeman, 2000b]. If the frequency were determined by phase locking between transmitter and receiver, as modeled by Schillen & König [1994] and Traub et al. [1996], the event would be manifested by increased coherence near zero phase difference between the transmitting and receiving sites.

This model led to the prediction that, when a rabbit was trained to respond to an odorant, a pre-stimulus 'search image' [Freeman, 1983] of the odor would be found in the spatial amplitude pattern of the bulbar EEG. The pattern would have a carrier frequency in the gamma range with a broad distribution of phase. By hypothesis, a poststimulus 'representational image' would have the same spatial amplitude pattern with decreased phase variance. Preliminary results from EEG in the olfactory bulb seemed to support this model [Fig. 10 in Freeman, 1980]. However, improved techniques of measurement of EEG amplitude and phase reduced the standard errors of measurement [Freeman & Viana Di Prisco, 1986]. New measurements revealed spatial patterns of phase (the phase cones) accompanying AM patterns, but not phase convergence [Freeman & Baird, 1987]. The reduction in phase dispersion seen earlier was traced to lowered EEG amplitude upon stimulus arrival. That lowering increased the coarse-graining of the amplitude measurement by truncation in analog-to-digital conversion (ADC), which inflated the correlation coefficient being used to estimate the cosine of the phase. This falsely decreased the phase dispersion. Following discovery of this artifact, the hypotheses of a representational 'search image' and of 'linear binding' in the olfactory system were rejected [Skarda & Freeman, 1987].

Neocortical EEG studies have likewise revealed phase cones that accompany AM patterns [Freeman & Barrie, 2000; Freeman & Rogers, 2002]. The cones have spatial diameters

comparable to the distances reported for synchronized unit activity [Singer & Gray, 1995], but the synchrony is not at zero lag. As predicted by the linear model, intercortical coherences, correlations and multiple correlation coefficients are maximal at zero lag, but only after digitizing, band pass filtering and spatial ensemble averaging. High correlations did not hold for individual signals [Kozma et al., 2001]. There were no increases in synchrony at the expected times of transmission and reception. There were no local increases in amplitude of activity ("bursts") in receiving areas at times predicted for increased synchrony of transmitting areas at zero lag or with predicted delays. Other shortcomings of the linear binding hypothesis have been described elsewhere [Tovée & Rolls, 1992; Hardcastle, 1994].

4.2. Exploration of differing mechanisms of cortical transmission and reception

Fourth and most important, the ionic mechanisms for transmission and reception of wave packets by cortex should be carefully distinguished. The operations of band pass temporal filtering and low pass spatial filtering may provide a mesoscopic mechanism for sending AM patterns not only from one cortex to another, but just as importantly into the basal ganglia and brain stem nuclei. The global AM patterns appear to be widely distributed over an entire hemisphere, and the corticothalamic and corticostriatal pathways have varying lengths and diameters of axons, despite the central locations of the basal ganglia with respect to the cortices. Intercortical transmission distances are still more varied. The wave forms in Fig. 4 show that gamma activity in many parts of the forebrain is not synchronized, but the high average levels of correlation among their EEGs at zero lag [Figs. 3 and 9] under these constraints indicate that covariance permeates each cerebral hemisphere continuously. The power of the operations of truncation (comparable in its effects to pulse frequency modulation), band pass filtering, and spatial ensemble averaging is shown by applying them to random numbers simulating noise. They largely replicate the correlations with zero mean lag. This relation may hold for all subcortical targets, irrespective of variation in their distances from multiple parts of the cortex.

Cortical transmission and reception both depend on gamma activity but in differing ways. These ways reflect two classes of neural mechanism that have been developed to explain the origin of gamma activity in the cerebral cortex. One is microscopic, the other mesoscopic. A strong case for the genesis of gamma by individual neurons, based on recordings from thalamus [Steriade et al., 1993; Gray & McCormick, 1996; Pedroarena & Llinás, 1997; König & Schillen, 1991] and hippocampal slices [Whittington et al., 2000], holds that repetitive firing is local and intrinsic to neurons, and can be facilitated by the kinetics of GABA_A conductances in the membranes of inhibitory neurons. An equally strong case for the origin of gamma by interactions among neurons in populations, based on recording from the olfactory system in waking animals, holds that oscillations in firing probability arise by distributed synaptic negative feedback between excitatory and inhibitory neurons [Freeman, 1975, 2000a]. A critical litmus test to determine which is responsible for observed instances of gamma is the phase relation between the excitatory and inhibitory neuronal firings. The microscopic model predicts that they fire in phase with zero lag between them [Traub et al., 1996]. The mesoscopic model predicts that the peak of firing of the inhibitory neurons lags that of the excitatory neurons by about a quarter cycle at the prevailing frequency [Freeman, 1975; Eeckman & Freeman, 1990; Ahrens & Freeman, 2001].

In both cases the oscillations require sustained excitation from internal or external sources, and they are manifested by fluctuations both in dendritic currents and rates of firing of participating neurons. Both models require the same four types of synaptic connections among the neurons: e-e, e-i, i-e and i-i, that are mediated by the same neurotransmitters. Both show the same inverse relation between amplitude and characteristic frequency of oscillation. In the microscopic model this relation is attributed to the receptor kinetics of the dendritic synapses, a microscopic property, whereas in the mesoscopic model it is attributed to reduced negative feedback gain, a mesoscopic property, when axons are driven below threshold during high intensity inhibition and are unable to transmit proportionate output [Freeman, 1975]. For transmission, the optimal

properties are spatial coherence of broad band oscillation and wide divergence of output, for which the mesoscopic mechanism is most effective. For reception, the optimal properties are narrow band tuning of local neural networks, for which microscopic mechanisms are more appropriate [Häusser et al., 2000]. These models are not in conflict; they address different hierarchical levels of organization and complementary aspects of communication.

The transmitting operations can be construed to be relatively fixed in respect to frequency by the anatomy and biophysics of cortical neurons, though the local amplitude of oscillation can be modified by conditioning to compensate for signal degradation by phase lags, perhaps under feedback control from receivers. In contrast, the tuning curves of receiving mechanisms may be subject to both rapid and long term adaptation by synaptic changes with learning. These may include cellular mechanisms of mutual inhibition [e.g. Traub et al., 1996; Buhl, Tamas & Fisahn, 1998; Whittington et al., 2000], that could tune receiving frequencies to selected transmitting frequencies in the broad gamma range, and also compensate for low correlations due to excessive phase lags. Such tuning would likely be under local homeostatic feedback control [Chang & Freeman, 1999; Freeman 1999b]. The techniques for testing this hypothesis are to stimulate afferent pathways with electrical paired shocks, determine a near linear range of cortical response [Biedenbach & Freeman, 1965], fit sums of linear basis functions to averaged impulse responses and poststimulus time histograms, design a cortical transfer function by use of the Fourier transform of the averaged evoked potential, and construct a linear feedback model in differential equations to evaluate the synaptic gains [Freeman, 1975, 2000a]. The analysis of evoked potentials is guided by spectral analysis of EEG [Boudreau & Freeman, 1963], measurement of d.c. potentials [Gonzalez-Estrada & Freeman, 1984], and calculation of firing probabilities of units conditional on the EEG amplitude and frequency [Eeckman & Freeman, 1990]. The gains are manipulated by pharmacological agents [Seyal, 1976], and by training subjects to discriminate different frequencies or other parameters of afferent electrical stimuli given as CS+ and CS-. The changes in synaptic gains are calculated from the model to

determine which synapses are changed with learning, in which directions, and at what times [Emery & Freeman, 1969; Freeman, 2000a].

ACKNOWLEDGMENTS

This work was funded by research grants from NIMH (MH06686), ONR (N63373 N00014-93-1-0938), NASA (NCC 2-1244), and NSF (EIA-0130352). We express our gratitude to A. Halperin, J. Leung, and L. Jennings for help with surgeries and post operative care, K. Ahrens and A. Smart for helping to rebuild the switchboard connecting the recording cable to the amplifiers, and P. German for assistance during training and recording.

REFERENCES

- Ahrens, K.F. & Freeman, W.J. [2001] Response dynamics of entorhinal cortex in awake, anesthetized and bulbotomized rats. *Brain Res.* **911**: 193-202
- Barrie, J.M., Freeman, W.J. & Lenhart, M.D. [1996] Spatiotemporal analysis of prepyriform, visual, auditory and somesthetic surface EEG in trained rabbits. *J. Neurophysiol.* **76**: 520-539.
- Biedenbach, M.A. & Freeman, W.J. [1965] Linear domain of potentials from the prepyriform cortex with respect to stimulus parameters. *Exper. Neurol.* **11**: 400-417.
- Boeijinga, P.H. & Lopes da Silva, F.H. [1988] Differential distribution of beta and theta EEG activity in the entorhinal cortex of the cat. *Brain Res.* **448**: 272-286.
- Boudreau, J.C. & Freeman, W.J. [1963] Spectral analysis of electrical activity in the prepyriform cortex of cat. *Exper. Neurol.* **8**: 423-430
- Brockwell, P. & Davis, R. [1991] *Time Series: Theory and Methods, 2nd ed.* (Springer-Verlag, London UK).
- Bruns, A., Eckhorn, R., Jokeit, H. & Ebner, A. [2000] Amplitude envelope correlation detects coupling among incoherent brain signals. *NeuroReport* **11**: 1509-1514.
- Buhl, E. H., Tamas, G. & Fisahn, A. [1998] Cholinergic activation and tonic excitation induce persistent gamma oscillations in mouse somatosensory cortex *in vitro*. *J. Physiol.* **513**: 117-126.
- Buzsáki, G. [1996] The hippocampal-neocortical dialogue. *Cerebral Cortex* **6**: 81-92.
- Chang, H.-J. & Freeman, W.J. [1999] Local homeostasis stabilizes a model of the olfactory system globally in respect to perturbations by input during pattern classification. *Intern. J. Bifurc. & Chaos* **8**: 2107-2123.
- Eckhorn, R., Bruns, A., Saam, M., Gail, A., Gabriel, A. & Brinksmeyer, H.J. [2001] Flexible cortical gamma-band correlations suggest neural principles of visual processing. *Visual Cogn.* **8**: 519-530.

- Eeckman, F.H. & Freeman, W.J. [1990] Correlations between unit firing and EEG in the rat olfactory system. *Brain Res.* **528**: 238-244.
- Emery, J.D. & Freeman, W.J. [1990] Pattern analysis of cortical evoked potential parameters during attention changes. *Physiol. & Behav.* [1969]**4**: 67-77.
- Freeman, W.J. [1975] *Mass Action in the Nervous System..* (Academic Press, New York).
- Freeman, W.J. [1979] EEG analysis gives model of neuronal template-matching mechanism for sensory search with olfactory bulb. *Biol. Cybern.* **35**: 221-234.
- Freeman, W.J. [1980] Use of spatial deconvolution to compensate for distortion of EEG by volume conduction. *IEEE Trans. Biomed. Engin.* **27**: 421-429.
- Freeman, W.J. [1983] The physiology of mental images. *Biol. Psychiat.* **18**: 1107-1125.
- Freeman, W.J. [2000a] *Neurodynamics. An Exploration of Mesoscopic Brain Dynamics.* (Springer-Verlag, London UK).
- Freeman, W.J. [2000b] Characteristics of the synchronization of brain activity imposed by finite conduction velocities of axons. *Intern. J. Bifurc. Chaos* , **10**: 2307-2322.
- Freeman, W.J. [2001] *How Brains Make Up Their Minds.* (Columbia U.P., New York).
- Freeman, W.J. [2003] A neurobiological theory of meaning in perception. Part 1. Information and meaning in nonconvergent and nonlocal brain dynamics. *Int. J. Bifurc. Chaos* 13: in press
- Freeman, W.J. & Baird, B. [1987] Relation of olfactory EEG to behavior: Spatial analysis. *Behav. Neurosci.* **101**: 393-408.
- Freeman, W.J. & Barrie, J.M. [2000] Analysis of spatial patterns of phase in neocortical gamma EEG in rabbit. *J. Neurophysiol.* **84**: 1266-1278.
- Freeman, W.J. & Grajski, K.A.[1987] Relation of olfactory EEG to behavior: Factor analysis. *Behav. Neurosci.* **101**: 766-777.
- Freeman, W.J. & Rogers, L.J. [2002] Fine temporal resolution of analytic phase reveals episodic synchronization by state transitions in gamma EEG. *J. Neurophysiol.* **87**, 937-945.

- Freeman, W.J. & Viana Di Prisco, G. [1986] Relation of olfactory EEG to behavior: Time series analysis. *Behav. Neurosci.* **100**: 753-763.
- Gaál, G. & Freeman, W.J. [1998] Relations among EEG from entorhinal cortex, olfactory bulb, somatomotor, auditory and visual cortices in trained cats. In: Ding, M., Ditto, W., Pecora, L., Spano, M. & Vohra, S., eds., *Proc. 4th Exper. Chaos Conf.* pp. 179-184. (World Scientific, Singapore).
- Gonzalez-Estrada, M.T. & Freeman, W.J. [1980] Effects of carnosine on olfactory bulb EEG, evoked potentials and D.C. potentials. *Brain Research.* **202**: 373-386.
- Gray, C.M. & McCormick, D.A. [1996] Chattering cells: superficial pyramidal neurons contributing to the generation of synchronous oscillations in the visual cortex. *Science* **274**: 122-129.
- Haig, A.R., Gordon, E., Wright, J.J., Meares, R.A. & Bahramali, H.B. [2000] Synchronous cortical gamma-band activity in task-relevant cognition. *NeuroReport* **11**: 669-675.
- Häusser, M., Spruston, N. & Stuart, G.J. [2000] Diversity and dynamics of dendritic signaling. *Science* **290**: 739-744.
- Hardcastle, V.G. [1994] Psychology's binding problem and possible neurobiological solutions. *J. Consciousness Studies* **1**: 66-90.
- Kay, L.M. & Freeman, W.J. [1998] Bidirectional processing in the olfactory-limbic axis during olfactory behavior. *Behav. Neurosci.* **112**: 541-553.
- König, P. & Schillen, T.B. [1991] Stimulus-dependent assembly formation of oscillatory responses. 1. Synchronization. *Neural Comp.* **3**: 155-166.
- Kozma R., Alvarado, M., Rogers, L.J., Lau, B. & Freeman, W.J. [2001] Emergence of uncorrelated common-mode oscillations in the sensory cortex. *Neurocomputing* **38-40**: 747-755.
- Lopes da Silva, F.H., Witter, M.P., Boeijinga, P.H. & Lohmann, A.H.M. [1990] Anatomic organization and physiology of the limbic cortex. *Physiol. Rev.* **70**: 453-511.
- Milner, P.M. [1974] A model for visual shape recognition. *Psychol. Rev.* **81**: 521-535.

- Pedroarena, C. & Llinás, R. [1997] Dendritic calcium conductances generate high-frequency oscillation in thalamocortical neurons. *Proc. Nat. Acad. Sci. USA*: 94: 724-728.
- Politis, D.N., Romano, J. & Lai, T. [1998] Bootstrap confidence intervals for spectra and cross-spectra. *IEEE Trans. Signal Proc.* **92**: 1206-1215.
- Schillen, T.B. & König, P. [1994] Binding by temporal structure in multiple feature domains on an oscillatory neuronal network. *Biol. Cybern.* **70**: 397-405.
- Seyal, M. [1976] *A neuropharmacological study of evoked potentials in the olfactory bulb*. Ph.D. Thesis in Physiology, University of California at Berkeley.
- Singer, W. & Gray, C.M. [1995] Visual feature integration and the temporal correlation hypothesis. *Ann. Rev. Neurosci.* **18**: 555-586.
- Skarda, C.A. & Freeman, W.J. [1987] How brains make chaos in order to make sense of the world. *Behav. Brain Sci.* **10**: 161-195.
- Steriade, M., Curró Diossi, R. & Contreras, D. [1993] Electrophysiological properties of intralaminar thalamocortical cells discharging rhythmic (40 Hz) spike-bursts at c.1000 Hz during waking and rapid eye movement sleep. *Neuroscience* **56**: 1-9.
- Stryker, M.P. [2001] Drums keep pounding a rhythm in the brain. *Science* **291**: 1506-1507.
- Tovée, M.J. & Rolls, E.J. [1992] The functional nature of neuronal oscillations. *Trends in Neurosciences* **15**: 387.
- Traub, R.D., Whittington, M.A., Stanford, I.M. & Jefferys, J.G.R. [1996] A mechanism for generation of long-range synchronous fast oscillations in the cortex. *Nature* **383**: 421-424.
- von der Malsburg, C. [1983] How are nervous structures organized? In: Basar, E., Flohr, H., Haken, H. & Mandell, A. J. (eds.), *Synergetics of the Brain*, Berlin: Springer, pp. 238-249.
- Whittington, M.A., Faulkner, H.J., Doheny, H.C. & Traub, R.D. [2000] Neuronal fast oscillations as a target site for psychoactive drugs. *Pharmacol. & Therap* **86**: 171-190.